Properties of thin films of isotactic polypropylene blended with polyisobutylene and ethylene–propylene–diene terpolymer rubbers

Ezio Martuscelli, Clara Silvestre and Liliana Bianchi
Istituto di Ricerche su Tecnologia dei Polimeri e Reologia del CNR, Arco Felice, Napoli, Italy
(*Received* 8 *October* 1982; *revised* 23 *December* 1982)

An experimental study was carried out to investigate the kinetic, morphological and thermodynamic properties of thin films of isotactic polypropylene (iPP) blended with several elastomers such as ethylene–propylene–diene terpolymer (EPDM) and three samples of polyisobutylene (PIB) with different molecular masses. The addition of the rubber to iPP causes drastic modifications in the morphology, nucleation density, spherulite growth rate and thermal behaviour of iPP. Such modifications depend strongly on the chemical and molecular mass of the added elastomer and on the composition of the blend. All the elastomers studied seem to act as nucleating agents for the iPP spherulites. The addition of PIB to iPP results in a reduction of the spherulite growth rate G, whereas the addition of EPDM does not seem to have a great influence. For the iPP/PIB_{HM}, iPP/PIB_{MM} and iPP/EPDM blends a depression of the equilibrium melting temperature T_m, with respect to that of pure iPP, is observed. This depression is increased for the blend containing 20% rubber. This effect is probably related to phenomena of partial miscibility in the melt and to the coexistence of processes such as molecular fractionation and preferential dissolution of the more defective molecules.

Keywords Isotactic polypropylene; polyisobutylene; ethylene–propylene–diene terpolymer; blends; crystallization; morphology

INTRODUCTION

During the last few years a great number of papers have been published on binary blends made of isotactic polypropylene (iPP) and elastomers with different chemical nature[1-7]. Such mixtures are of tremendous interest for both technological and scientific reasons.

In fact, on the one hand, it is enough to add to iPP small quantities of ethylene–propylene copolymers (EPM), ethylene–propylene–diene terpolymer (EPDM), butyl rubber (BR), styrene–butadiene–styrene copolymer (SBS), polyisobutylene (PIB), etc., to obtain an interesting improvement of the impact strength and of the environmental stress cracking resistance of the iPP at low temperature. On the other hand, to get a better understanding of the mechanical behaviour of these blends, it is necessary to investigate in detail the crystallization process from the melt and the morphology that emerges during the crystallization of the mixtures.

In this paper the isothermal crystallization, morphology and melting behaviour of thin films of isotactic polypropylene blended with an ethylene–propylene–diene terpolymer and three samples of polyisobutylene with different molecular masses are investigated.

The main goal of the research is to study in detail how the blend composition, chemical structure and molecular mass of the elastomer may influence:

(i) the crystallization of isotactic polypropylene from the melt (radial growth rate of spherulites and nucleation density);

(ii) the overall morphology of the binary mixtures (shape, size and structure of the spherulites of the crystallizable component and of the rubbery domains);

(iii) the thermal behaviour of the iPP (enthalpy of fusion, observed melting temperature and equilibrium melting temperature).

The results will be compared with those reported in a previous paper[1] which deals with the morphology, crystallization and melting behaviour of films of iPP blended with three ethylene–propylene copolymers having different ethylene contents.

EXPERIMENTAL

Materials

The molecular characteristics together with the sources and trade names of the polymers used in the present investigation are reported in *Table 1*.

Before blending, all the polymers were purified by using the following procedure: they were first dissolved in xylene at 120°C and washed with HCl (water solution, 10% volume); then they were precipitated with methanol under strong agitation, washed with acetone and finally dried under vacuum at 80°C for 12 h.

0032-3861/83/111458-11$03.00

Table 1 Molecular characteristics, sources and trade names of the polymers used in the present investigation

Polymer	Source and trade name	Molecular mass
Isotacticpolypropylene (iPP)	RAPRA	$\overline{M}_w = 3.07 \times 10^5$ $\overline{M}_n = 1.56 \times 10^4$
Polyisobutylene (PIB)	Vistanex LM · MH (Esso) (PIB_{LM})	$\overline{M}_v = 6.6 \times 10^4$
	Vistanex L120 (PIB_{MM})	$\overline{M}_v = 1.6 \times 10^6$
	EGA Chemie (PIB_{HM})	$\overline{M}_v = 3.5 \times 10^6$
Ethylene–propylene–diene terpolymer (EPDM)	Dutral TER 054-E (Montedison)	

Preparation of the blends

Binary blends of iPP/elastomers were prepared by first dissolving the two components in xylene at 120°C in the desired proportions; then the solvent was rapidly evaporated by using a Rotovapor and the resulting powder dried under vacuum to eliminate any trace of residual solvent.

Thin films (about 10 μm thick) were obtained by compression moulding of the blend powder at 200°C.

Radial growth rate and melting temperature measurements

The radial growth rates $G = dr/dt$ (r = radius of spherulites, t = time) were calculated by measuring the size of iPP spherulites as a function of time during the isothermal crystallization process. An optical polarizing microscope fitted with an automatized hot stage was used for the measurements. This standard procedure was followed: Blend films were sandwiched between a microscope slide and a cover glass, heated at 20°C above the melting point of iPP and kept for 10 min at this temperature. Then the temperature was suddenly lowered to the desired T_c and the sample allowed to crystallize isothermally. The radial growth of a spherulite focused upon was finally monitored during crystallization, taking photomicrographs at appropriate intervals of time. From the measured radius r, plotted against the time t, the radial growth rate G was calculated as the slope of the resulting straight lines. The observed melting temperature T'_m of iPP crystallized from melt blends was measured by heating the sample until birifringence disappeared. The corresponding temperature was taken as the observed melting point of the sample, T'_m.

RESULTS AND DISCUSSION

Overall morphology

In a previous paper[1] it was reported that EPM elastomers are ejected during the crystallization of iPP. A more careful analysis showed that the morphology is much more complex. In fact, it was possible to observe that the growth of iPP spherulites causes the ejection of EPM particles only for a short distance; then occlusion occurs on increasing the radius of the spherulites[2].

The analysis of optical micrographs of thin films of iPP/PIB blends shows that the overall morphology is dependent on the composition and on the molecular mass of the elastomer.

iPP/PIB_{LM} blends. Micrographs of films of iPP/PIB_{LM} blends are reported in *Figure 1*. In the case of 90/10 blends the elastomer is ejected, during crystallization, mainly at the growing spherulite boundaries. For the 80/20 blend the iPP spherulites are more open and coarse, suggesting that part of the elastomer is probably incorporated in interlamellar regions. The overall morphology of blends with a higher elastomer content is more complicated as interconnected rubbery domains are observed.

iPP/PIB_{MM} blends. In such blends (see *Figure 2*), for all composition and T_c explored, the elastomer separates from the iPP phase, forming spherical domains incorporated in intraspherulitic regions.

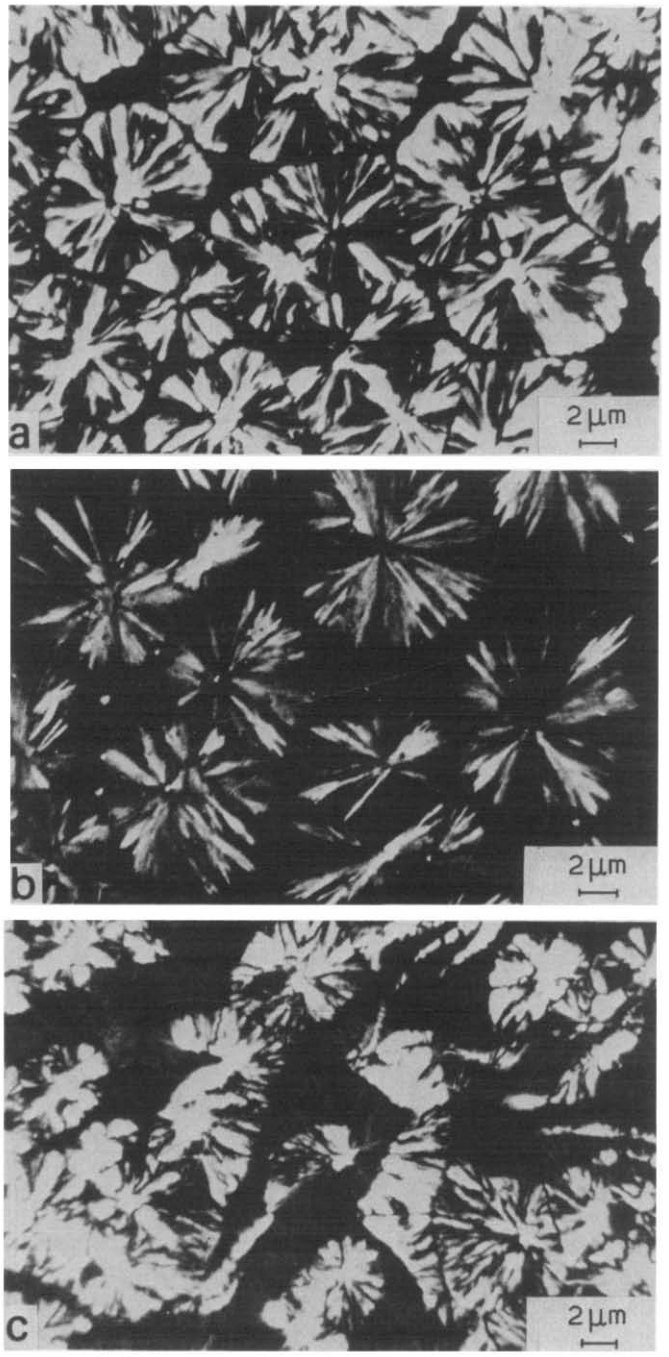

Figure 1 Optical micrographs of melt crystallized films of iPP/PIB_{LM} blends, T_c = 131°C, crossed polarizers: (a) 90/10, (b) 80/20, (c) 60/40

iPP/PIB$_{HM}$ blends. In films of iPP/PIB$_{HM}$ 90/10 blend (see *Figure 3*), the elastomer is mainly ejected at the spherulite boundaries and probably also in interlamellar regions as the spherulites, especially at the borders, are more open and coarse. In the case of the 80/20 blend, spherical elastomeric domains in both intra- and interspherulitic regions are observed. Interconnected morphology is found in blends with higher PIB$_{HM}$ content (see *Figure 3*).

The observation that PIB$_{LM}$ is ejected mainly in interspherulitic regions, in contrast to what happens to the PIB$_{MM}$ and PIB$_{HM}$, may be accounted for by the higher diffusivity coefficient of this rubber due to its relatively lower molecular mass.

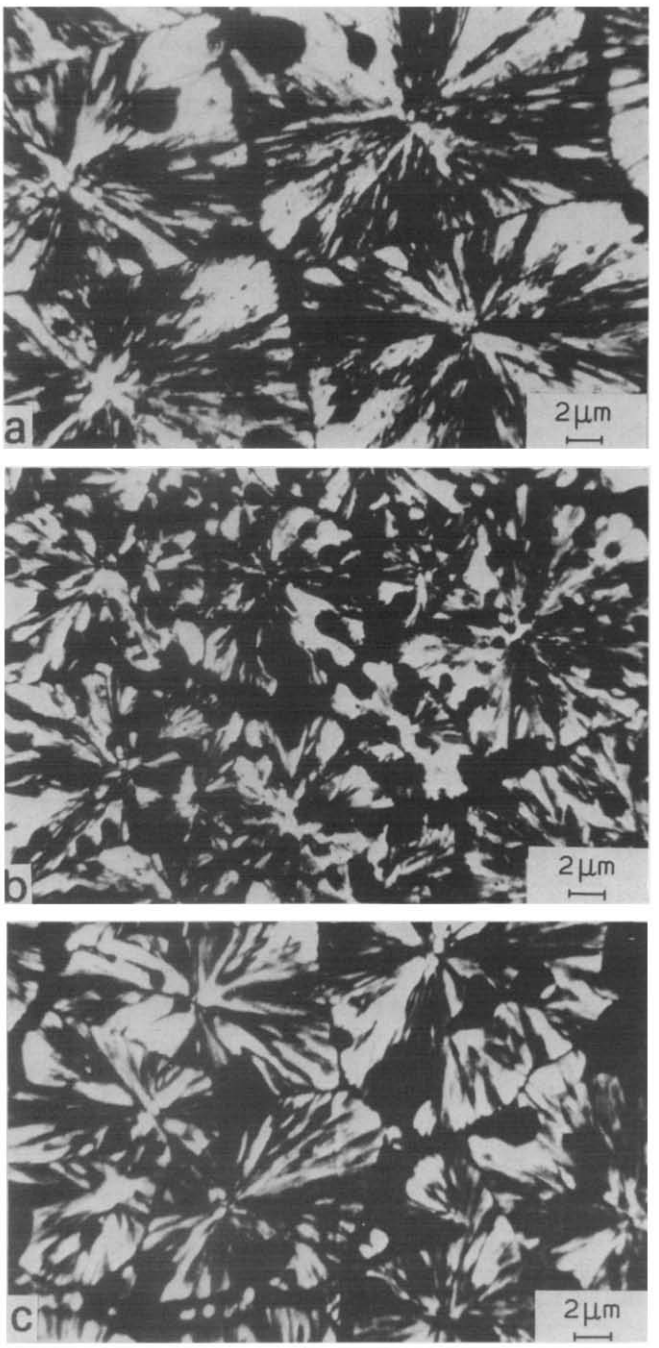

Figure 2 Optical micrographs of melt crystallized films of iPP/PIB$_{MM}$ blends, T_c = 131°C, crossed polarizers: (a) 90/10, (b) 80/20, (c) 60/40

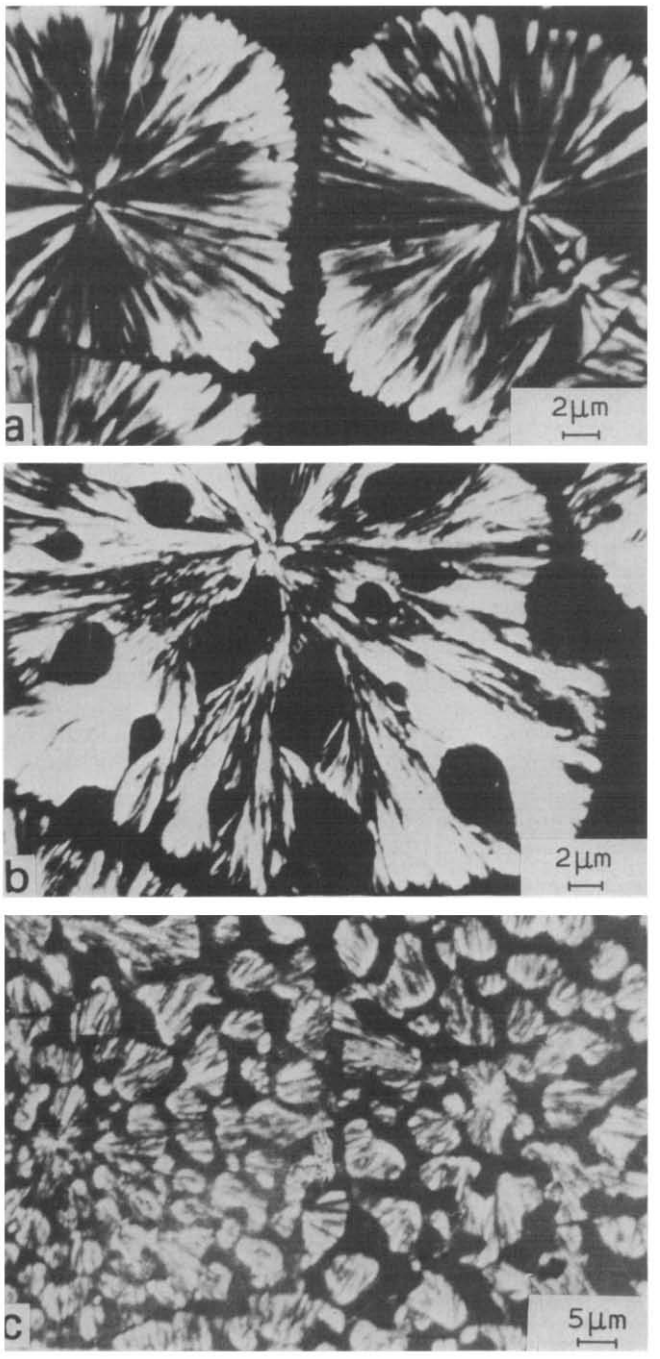

Figure 3 Optical micrographs of melt crystallized films of iPP/PIB$_{HM}$ blends, T_c = 135°C, crossed polarizer: (a) 90/10, (b) 80/20, (c) 60/40

iPP/EPDM blends. Optical micrographs of thin films of iPP/EPDM, reported in *Figure 4*, show that the elastomer separates in droplet-like domains mainly dispersed in intraspherulitic regions. As can be observed, these rubbery domains seem to be aligned along the radial direction.

Nucleation density: number of spherulites per unit area (N/S)

The addition of elastomers to iPP strongly influences the *N/S* values. The type of effect and its existence depend on the chemical nature and molecular mass of the elastomer, crystallization temperature and composition.

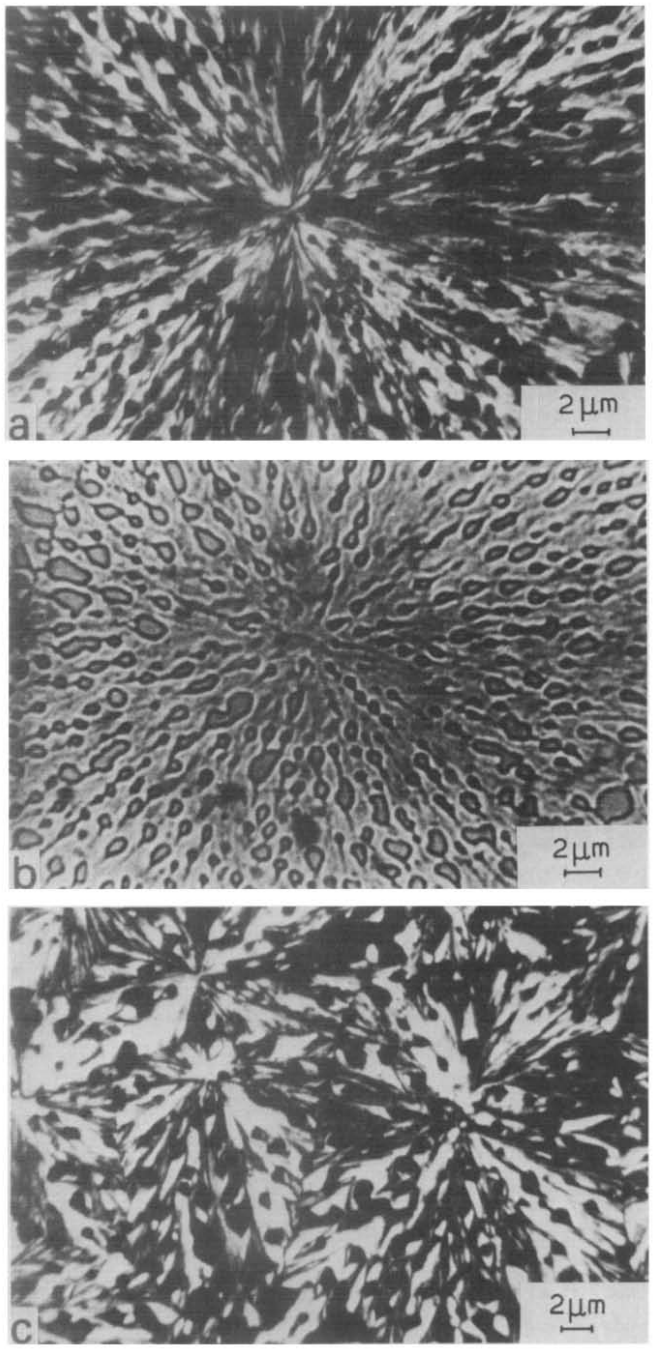

Figure 4 Optical micrographs of melt crystallized films of iPP/EPDM blends, T_c = 135°C: (a) 90/10, crossed polarizers; (b) 90/10, parallel polarizers; (c) 60/40, crossed polarizers

For iPP/EPDM blends, N/S increases monotonically with the percentage of rubber, as shown in *Figure 5*. For comparison on the same figure plots of N/S *versus* percentage of elastomer for iPP/EPM blends[1] are also reported. In such mixtures we observe that for the same T_c and blend composition N/S increases with the increase of the ethylene content of the elastomer and with the decrease of the molecular mass[1].

In the case of iPP/PIB blends, plots of N/S against the elastomer percentage show a maximum for the 90/10 blend composition. These synergistic effects, dramatic for the iPP/PIB_{LM} 90/10 blend (see *Figure 6*), are at the moment not easily interpreted. All blends show that for a given composition N/S decreases with the increase of T_c, in accord with the finding that for heterogeneous nucleation the nucleation density decreases when the supercooling diminishes.

The above observations strongly suggest that the elastomers may work as effective nucleating agents. This nucleation efficiency of the elastomers seems to depend on factors such as: chemical structure and molecular mass, composition and we believe also molecular mass distribution.

From the results reported above, it may be concluded that the overall morphology of blends of iPP and a non-crystallizing elastomer depends to a considerable extent on the composition and on the chemical structure of the amorphous component, as well as on their molecular mass.

At this point it is interesting to point out that the addition of rubbers to iPP causes drastic changes in some very important morphological factors of the semicrystalline matrix such as shape, dimension and structure of spherulites and interspherulitic boundaries.

All these factors, as shown by Friedrich[8], have a great influence on crack propagation and impact behaviour of pure iPP. Thus any theory elaborated to predict and to explain the fracture mechanism behaviour of iPP/rubber blends should take into account the fact that the matrix undergoes deep structural and morphological modifications following the addition of a rubbery component.

Spherulite radial growth rate

The addition of EPDM terpolymer to iPP at a given T_c causes only a small depression of G (see *Figure 7*). Similar behaviour was observed in the case of iPP/EPM blends[1]. In the case of iPP/PIB blends, G is influenced much more by composition and molecular mass of the elastomer. In fact, in such blends a large depression effect can be seen, as

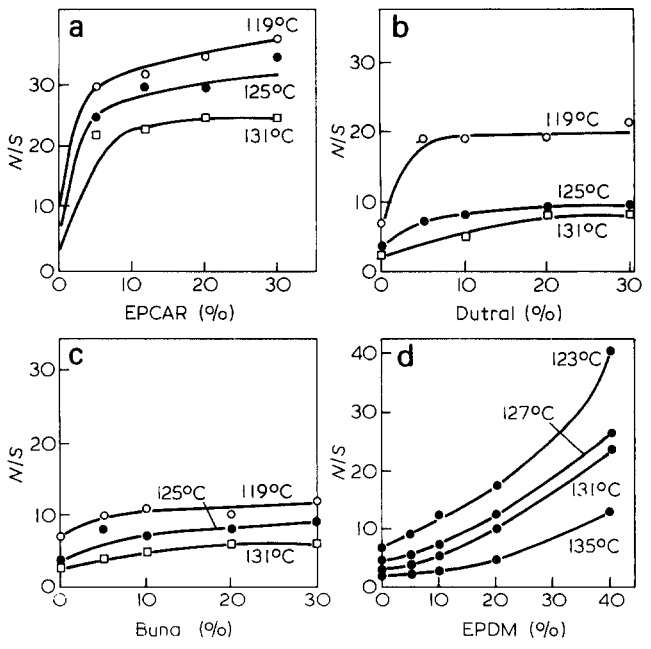

Figure 5 Number of spherulites per unit area, N/S, as a function of elastomer content at different T_c: (a) iPP/EPCAR blends, (b) iPP/Dutral blends, (c) iPP/Buna blends, (d) iPP/EPDM blends

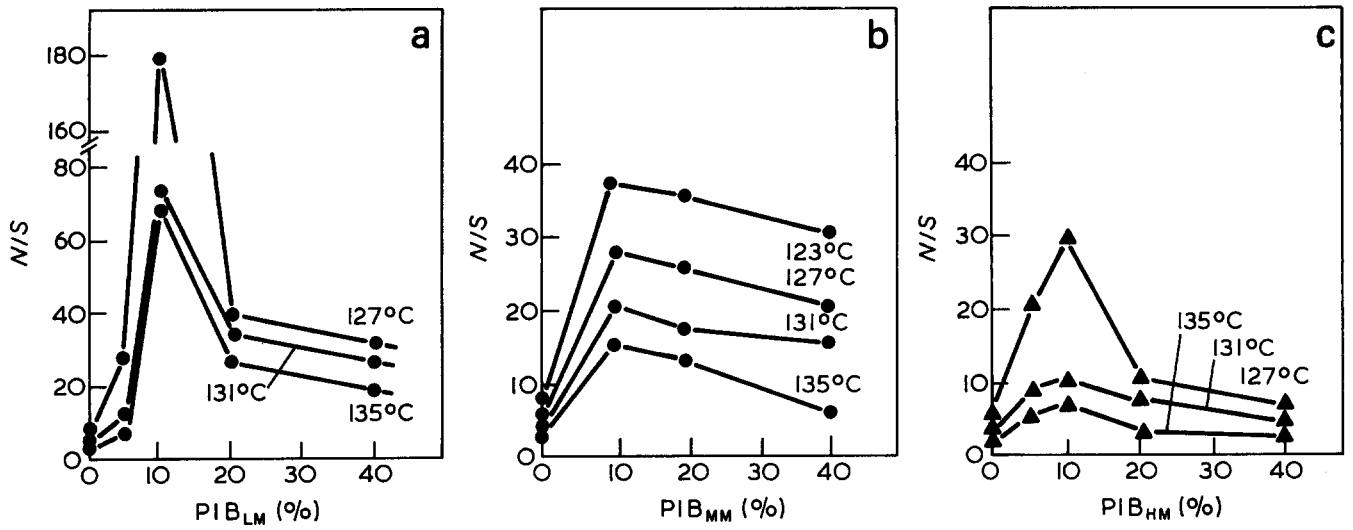

Figure 6 Number of spherulites per unit area, *N/S*, as a function of elastomer content at different T_c: (a) iPP/PIB$_{LM}$ blends, (b) iPP/PIB$_{MM}$ blends, (c) iPP/PIB$_{HM}$ blends

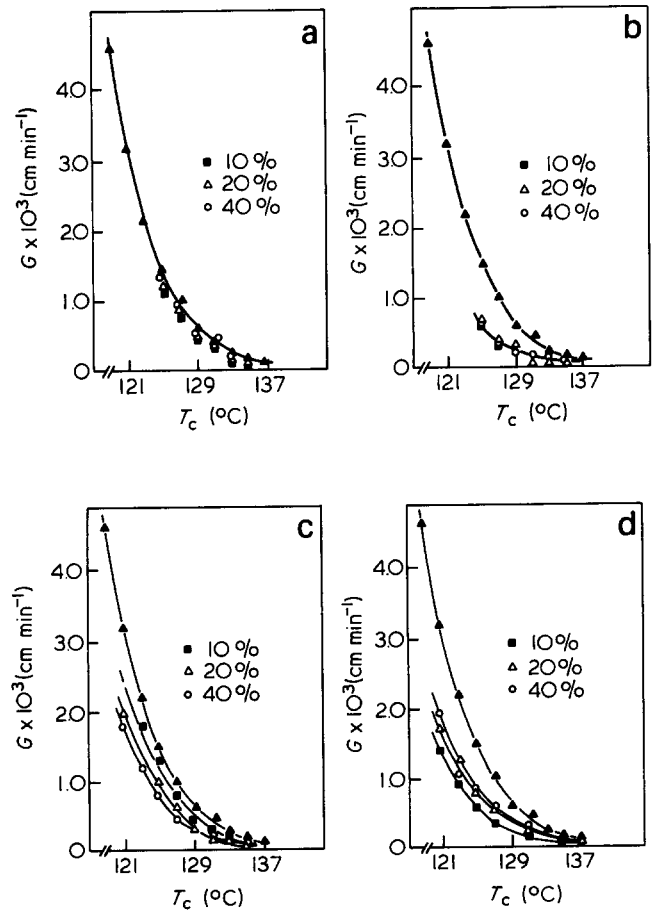

Figure 7 Radial growth rate, $G \times 10^3$ (cm min^{-1}), as a function of crystallization temperature, T_c (°C), at different compositions of added elastomer: (a' iPP/EPDM blends, (b) iPP/PIB$_{LM}$ blends, (c) iPP/PIB$_{MM}$ blends, (d) iPP/PIB$_{HM}$ blends

shown in *Figure 7*, whose existence is dependent on T_c and on the molecular mass of added PIB.

The variation of *G versus* composition, for iPP/EPDM and iPP/PIB blends, at a given T_c is shown in *Figure 8*. In the case of iPP/PIB blends the trend is dependent on the molecular mass of PIB. It can be observed that for iPP/PIB$_{MM}$ blends at a given T_c, *G* decreases monotonically with the elastomer content, whereas plots of *G versus* composition for iPP/PIB$_{HM}$ show a minimum at a 90/10 blend composition. In the case of iPP/PIB$_{LM}$, after an initial drop *G* keeps almost constant with increase of the rubber content.

Interesting effects are observed when the values of *G* of iPP, iPP/PIB, iPP/EPDM and iPP/EPM blends are compared at the same undercooling ΔT (ΔT is defined as $T_m - T_c$). Plots of *G versus* the percentage of elastomer in

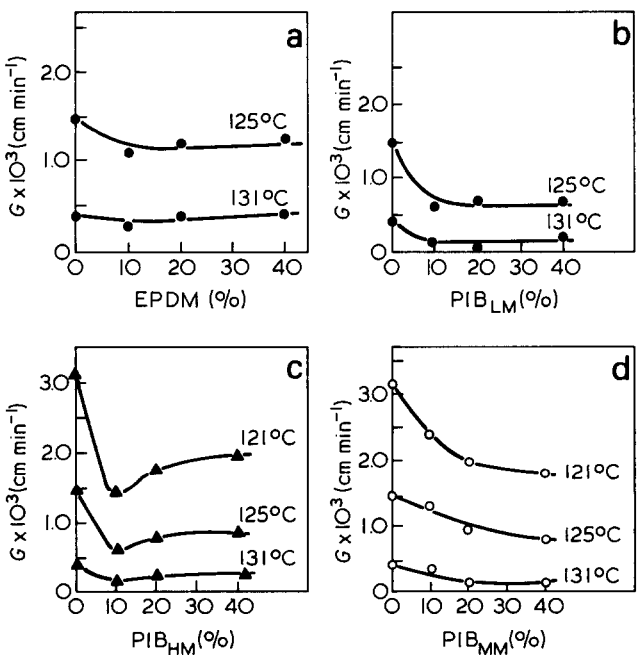

Figure 8 Radial growth rate, $G \times 10^3$ (cm min^{-1}), as a function of elastomer content at different T_c: (a) iPP/EPDM blends, (b) iPP/PIB$_{LM}$ blends, (c) iPP/PIB$_{MM}$ blends, (d) iPP/PIB$_{HM}$ blends

the case of iPP/PIB_{MM}, iPP/PIB_{HM} and iPP/EPDM at ΔT = constant show maxima (see *Figure 9*), more pronounced at higher ΔT, for an elastomer content of about 20%. In contrast, a minimum for 10% of rubber is observed on the plots of *g versus* percentage of elastomer for iPP/PIB_{LM} blends (see *Figure 9*).

A depression in G is observed in the case of iPP/EPM blends if the values are compared at constant ΔT. The trend of G *versus* percentage of EPM at constant ΔT as shown in *Figure 10* is dependent on the type of copolymer used as second component. It should be noted that the error on G values has been calculated as 0.02×10^{-3} cm min^{-1}.

For a polymer/diluent system the temperature dependence[9-11] of G may be accounted for by the following equation:

$$\log G - \log v_2 - \frac{\Delta F^*}{2.3RT_c} - \frac{2\sigma T_m \ln v_2}{b_0 \Delta H \Delta T}$$

$$= \log G_0 - \frac{\Delta\phi^*(\text{cryst. comp.})}{2.3RT_c} \qquad (1)$$

where ΔF^* is the activation free energy for the transport process at the liquid–solid interface, and $\Delta\phi^*$(cryst. comp.) is the free energy relative to the formation of a nucleus of critical size, when the system is constituted only by the crystallizable component.

Equation (1) fits the experimental data for the iPP/PIB blends quite well, in fact plots of the term on the left against $T_m/T_c\Delta T$ give straight lines. From the intercepts and the slopes it was possible to calculate, at every composition, the values of the folding surface free energy σ_e and of $\log G_0$. It should be noted that in the calculation[1] of ΔF^* the T_g of the blends was assumed equal to that of pure iPP ($T_g = -18°C$)[12] and the volume fractions were calculated by using density values measured at 180°C ($\rho_{iPP} = 0.766\ g\ cm^{-3}$; $\rho_{PIB} = 0.839\ g\ cm^{-3}$)[13,14].

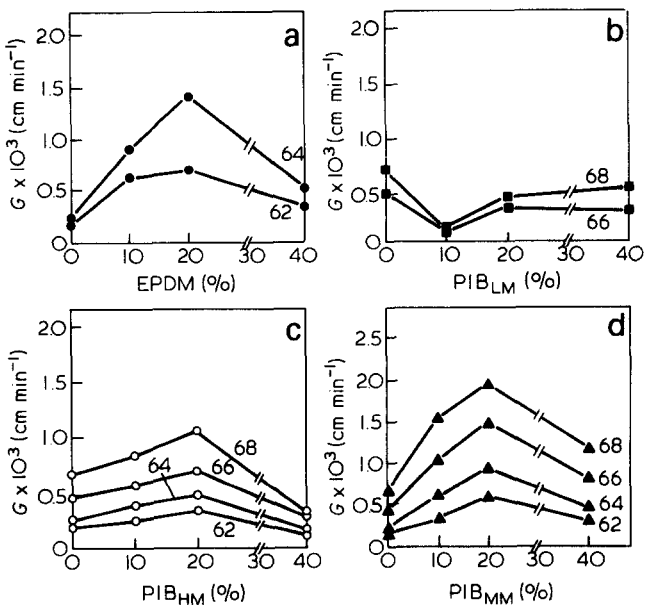

Figure 9 Radial growth rate, $G \times 10^3$ (cm min^{-1}, as a function of elastomer content at different undercooling ΔT ($T_m - T_c$): (a) iPP/EPDM blends, (b) iPP/PIB_{LM} blends, (c) iPP/PIB_{MM} blends, (d) iPP/PIB_{HM} blends

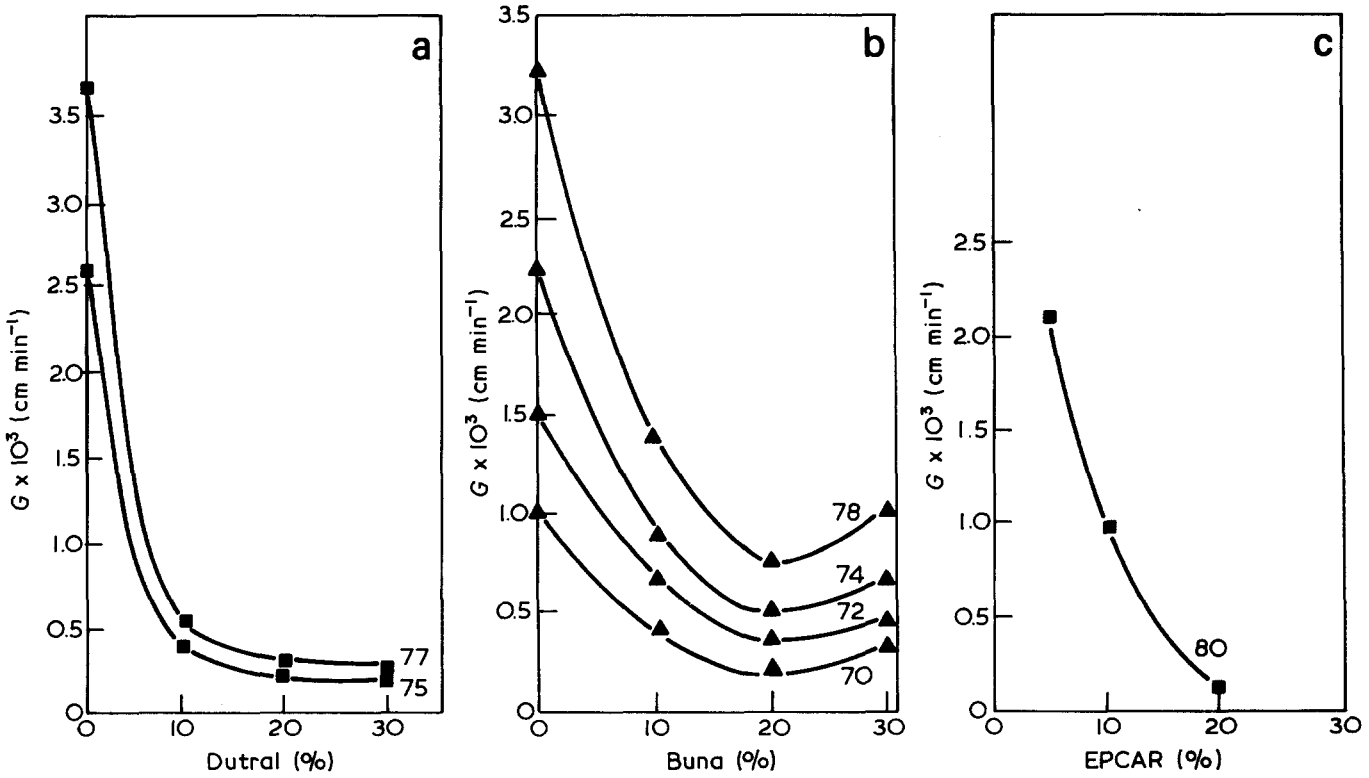

Figure 10 Radial growth rate, $G \times 10^3$ (cm min^{-1}), as a function of elastomer content at different undercooling ΔT ($T_m - T_c$): (a) iPP/Dutral blends, (b) iPP/Buna blends, (c) iPP/EPCAR blends

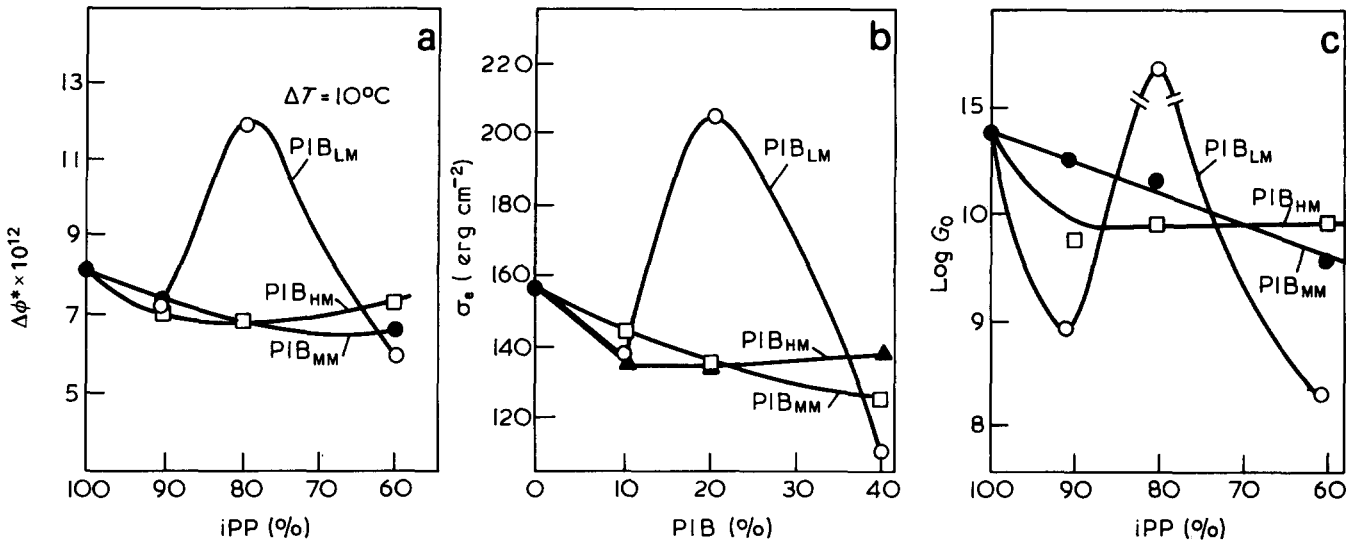

Figure 11 Composition dependence of (a) the free energy of formation $\Delta\phi^*$ of a nucleus of critical size, (b) the free energy of folding σ_e, and (c) pre-exponential factor, log G_0, for the iPP/PIB blends

Calculations performed by using for T_g of blends the values obtained from the Fox equation[15] indicate almost no variations in the values of σ_e and $\Delta\phi^*$. This last observation is accounted for by the fact that at low undercooling the transport term is less important if compared with the thermodynamic one.

The dependence of the free energy of formation of a nucleus of critical size $\Delta\phi^*$ and of the free energy of folding σ_e on the composition is shown in *Figure 11* for iPP/PIB blends. For iPP/PIB$_{MM}$ and iPP/PIB$_{HM}$ blends those quantities are slightly depressed in respect to that of pure iPP. In the case of blends of iPP with lower molecular mass PIB the plots of $\Delta\phi^*$ and σ_e *versus* composition present a maximum at about an 80/20 composition. The same trend of $\Delta\phi^*$ and σ_e is observed for the pre-exponential factor log G_0.

In the case of iPP/EPCAR and iPP/Dutral blends, $\Delta\phi^*$, σ_e and log G_0 increase with the percentage of rubber. In blends of iPP with Buna and EPDM terpolymers, these quantities present a maximum and a minimum respectively (see *Figure 12*).

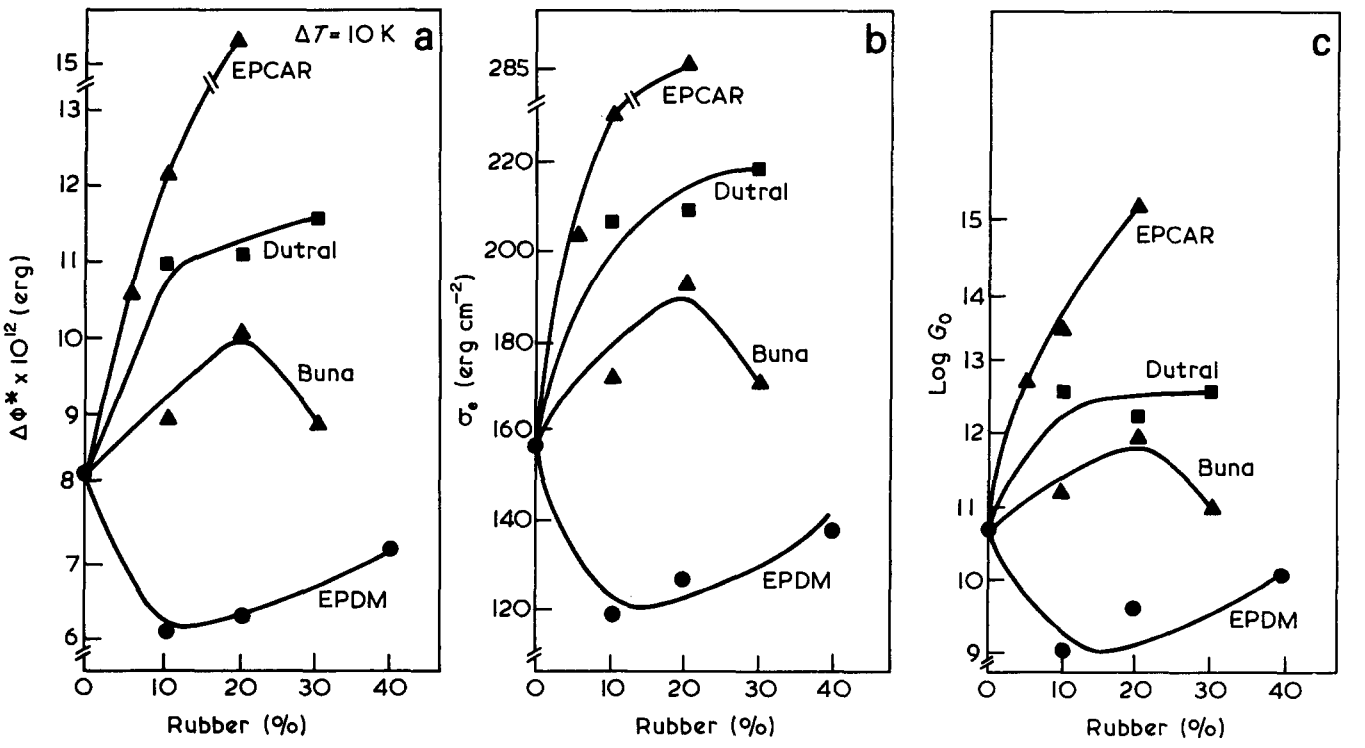

Figure 12 Composition dependence of (a) the free energy of formation $\Delta\phi$ of a nucleus of critical size, (b) the free energy of folding σ_e, and (c) the pre-exponential factor, log G_0, for the iPP/EPM and iPP/EPDM blends

Melting behaviour

In all blends investigated the observed melting temperature T'_m of pure iPP and iPP crystallized from iPP/elastomer mixtures increases linearly with T_c according to the relation of Hoffman[16]. The experimental error on the T'_m values is about ± 0.02°C (see *Figure 13*). In fact the experimental data may be fitted by the equation[17]:

$$T'_m = \frac{1}{\gamma} T_c + \left(1 - \frac{1}{\gamma}\right) T_m$$

where T_m is the equilibrium melting temperature and γ is the so-called 'morphological factor'. The values of γ for all blends are reported in *Table 2*. From this Table it is possible to point out that the morphological factor turns out to be almost independent of composition and of chemical nature of the elastomer, in analogy with the results obtained for the iPP/EPM blends[1]. Thus it may be concluded according to Nishi and Wang[18] that almost no kinetic effects on T_m and G are present. At a given T_c the observed melting temperatures of iPP/PIB blends are always lower than that of pure iPP. For iPP/PIB_{LM} and iPP/PIB_{MM} blends T'_m decreases monotonically with elastomer content, while a minimum is observed in iPP/PIB_{HM} blends at the 90/10 composition (*Figure 14*).

The variation of the equilibrium melting temperature T_m, obtained from the Hoffmann equation, with the elastomer percentage is shown in *Figure 15*. For iPP/PIB_{HM} and iPP/PIB_{MM} blends the T_m *versus* percentage of elastomer curves present a minimum for the 80/20 composition (the iPP/PIB_{HM} 60/40 blend has a value of T_m that is very close to that of pure iPP). Such behaviour may probably be accounted for if:

(1) both PIB_{MM} and PIB_{HM} are able to act as a diluent for iPP at lower concentrations;

(2) in blends with 20% of PIB, the mutual solubility of the two components in the melt decreases with increase of the elastomer content.

Table 2 Values of the morphological factor γ for the pure iPP and for the blends

Polymer	γ
iPP	2.04
iPP/EPDM	
10%	2.08
20%	2.22
30%	2.08
40%	2.00
iPP/PIB_{LM}	
10%	1.79
20%	1.85
30%	1.89
40%	1.89
iPP/PIB_{MM}	
10%	2.00
20%	2.1
30%	2.00
40%	1.92
iPP/PIB_{HM}	
10%	1.85
20%	2.00
30%	1.89
40%	1.85

In the case of iPP/PIB_{LM} blends the T_m *versus* percentage of PIB curve presents a maximum at a 90/10 composition.

Blends with higher PIB_{LM} content (>20%) have positive values of the equilibrium melting-point depression

$$\Delta T^\circ_m = T^\circ_m(\text{iPP}) - T_m(\text{blend})$$

The maximum in T_m is probably related to the fact that the PIB_{LM} is able to dissolve selectively a certain amount of the more defective iPP molecules, in analogy with what we found for EPM copolymers[1]. At a higher PIB_{LM}

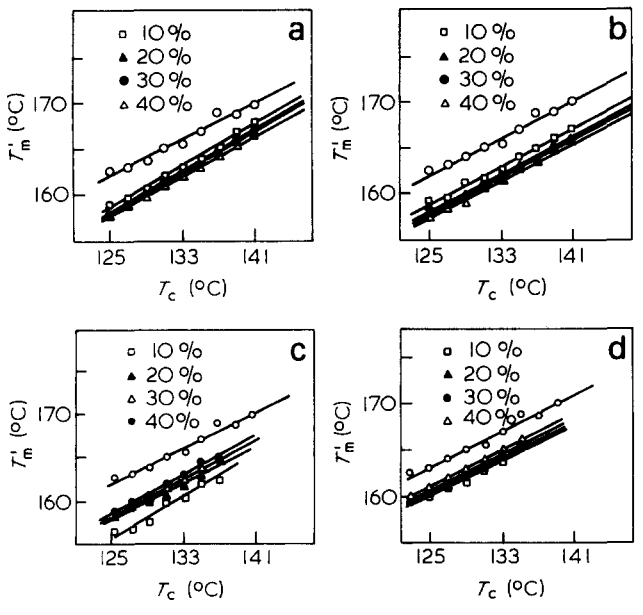

Figure 13 Variation of the observed optical melting temperature T'_m with crystallization temperature T_c, at constant composition: (a) iPP and iPP/PIB_{LM} blends, (b) iPP and iPP/PIB_{MM} blends, (c) iPP and iPP/PIB_{HM} blends, (d) iPP and iPP/EPDM blends

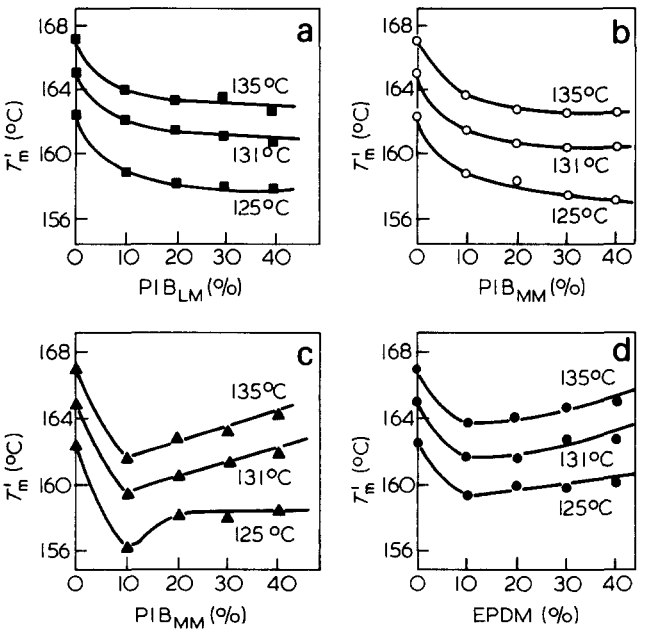

Figure 14 Observed optical melting temperature T'_m as function of the elastomer content at constant crystallization temperature T_c: (a) iPP/PIB_{LM} blends, (b) iPP/PIB_{MM} blends, (c) iPP/PIB_{HM} blends, (d) iPP/EPDM blends

content, ΔT_m° presumably becomes positive as the diluent effects prevail. Kinetic effects could be also present.

iPP/EPDM blends present a minimum in the T_m *versus* percentage of EPDM plot at an 80/20 composition (see *Figure 15*). Thus iPP/EPDM blends behave qualitatively as iPP/PIB_{HM} blends. Then the same considerations apply to the interpretation of their thermal behaviour.

It is interesting to point out that, as reported in a previous paper[1], the addition of EPM to iPP causes an elevation of the T_m and T'_m of the crystallizable component. The existence of this effect, measured in terms of the values of the equilibrium melting temperature depression ΔT_m°, is dependent on the molecular structure and molecular mass of the EPM copolymers. A larger increase in T_m and T'_m was observed for blends containing EPCAR, i.e. the copolymer with higher ethylene content and with lower molecular mass.

Thus it is possible to observe that the nature, molecular structure and mass of the elastomer used as the second component also determine thermal and melting behaviour of iPP/rubber blends.

A qualitative analysis of the melting-point depression for blends whose components are miscible in the molten state, as presented by several authors[18-20], by using the Flory–Huggins theory[17], gives the following equation for the equilibrium melting temperature depression:

$$\Delta T_m^\circ = -T_m^\circ(V_{2u}/\Delta H_{2u})Bv_1^2 \qquad (2)$$

In the case of iPP/PIB_{LM}, iPP/PIB_{MM}, iPP/PIB_{HM} and iPP/EPDM blends, the dependence of ΔT_m° on v_1^2 is not in agreement with the above relation, as can be seen by *Figure 16*. (Note that the data are limited to composition lower than 20% of rubber.)

The observed behaviour of ΔT_m° suggests that:

(1) the entropic contribution to ΔT_m° is not negligible;

(2) the X_{12} parameter depends on composition;

(3) the amount of rubber which acts as a diluent is lower than that added to iPP because of phase separation phenomena in the melt.

One approach to the theory of miscibility of polymers is

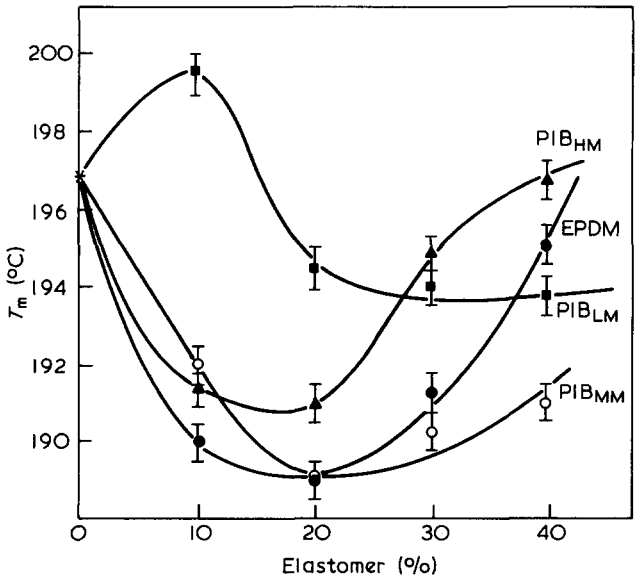

Figure 15 Variation of equilibrium melting temperature T_m with the elastomer percentage

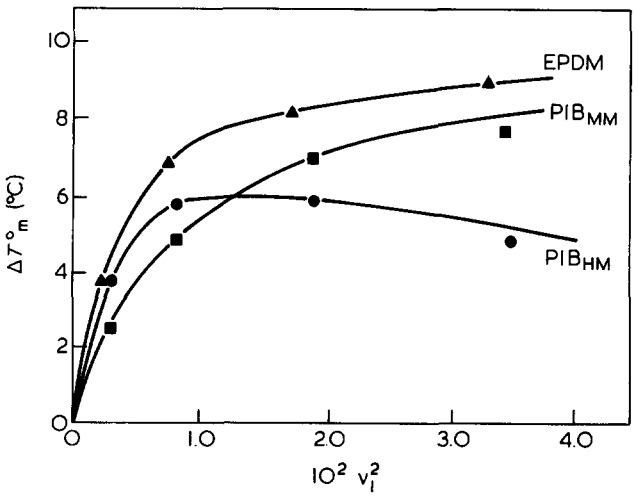

Figure 16 Dependence of ΔT_m on $v_1^2 \times 10^2$ for iPP/PIB_{MM}, iPP/PIB_{HM} and iPP/EPDM blends

based on the solubility parameter. The solubility parameter δ is usually defined as the square root of the vaporization energy (ΔE) per unit volume. According to such a theory the probability for two polymers to be compatible is high if they have similar solubility parameter values[21,22]. Calculation of the solubility parameter may be done by using the following equation:

$$\delta = \rho \frac{\sum F_i}{M}$$

where ρ is the density of the polymer at the wanted reference temperature, M is the molecular mass of the repetitive units of the polymer and $\sum F_i$ is the sum of the molar attraction constants of all the chemical groups of the repetitive units. Using literature equations for the temperature dependence of density of PIB[13] and iPP[14] amorphous phase, and calculating the attraction constant by means of the Hoy table[23], it is possible to report the values of δ as a function of T for the two polymers.

Figure 17 shows that the δ values for PIB and iPP are very close, with an almost constant difference of about 0.20 $(\text{cal cm}^{-3})^{1/2}$ in the 100°–200°C range of temperature. This result leads to the conclusion that it is likely that the iPP and PIB present in the melt have a certain degree of compatibility when they are blended together. This observation may explain some of our experimental data, i.e. depression in the T_m and G values, at least for compositions not exceeding 20–30% of PIB.

DISCUSSION AND CONCLUSIONS

The type of dependence on composition, crystallization temperature and chemical nature and molecular mass of the components observed in kinetic and thermodynamic quantities relative to the isothermal crystallization process of crystallizable mixtures, the final overall morphology and the melting behaviour are to be related to the physical state of the melt, which at T_c is in equilibrium with the solid phase which is developing.

Let us assume that the binary blend with only one crystallizable component presents a phase diagram in the melt characterized by a lower critical solution temperature behaviour. Then the possibilities that should be considered at least in principle are illustrated schemati-

cally in *Figure 18*. As shown in this Figure the equilibrium melting temperature of the crystallizable component A may be lower or higher than the critical temperature T_{cr}.

Compatibility of the components at all T_c *and compositions explored:* $T_m < T_{cr}$, $T_c < T_{cr}$ *(see Figure 18a)*

The solid phase grows in thermodynamic equilibrium with a homogeneous liquid phase. The non-crystallizable component acts as a diluent, thus leading to a depression of the observed and equilibrium melting point.

Regarding the radial growth rate of the spherulites, the presence of a diluent should influence both the transport term ΔF^* and the thermodynamic term $\Delta\phi^*$ which appear in equation (1). The effect of diluent on ΔF^* is related to the fact that a mixture of compatible polymers presents only one glass transition temperature T_g intermediate between those of the pure components.

However, according to whether or not the T_g of the crystallizable component is higher or lower than that of the uncrystallizable component, and taking into account the WLF expression[10], the following two possibilities may be observed:

(1) T_g(blend) < T_g(cryst. comp.)
ΔF^*(blend) < ΔF^*(cryst. comp.)
$\rightarrow G$(blend) > G(cryst. comp.)

(2) T_g(blend) > T_g(cryst. comp.)
ΔF^*(blend) > ΔF^*(cryst. comp.)
$\rightarrow G$(blend) < G(cryst. comp.)

The effect of the diluent on $\Delta\phi^*$ may be accounted for by considering the expression for the free energy of formation of a nucleus of critical size for a polymer/diluent system:

$$\Delta\phi^*(\text{blend}) = \Delta\phi^*(\text{cryst. comp.}) - \frac{2\sigma_e k T_m T_c}{b_0 \Delta H \Delta T} \ln v_2$$

As the term $-2\sigma_e k T_m T_c (\ln v_2)/b_0 \Delta H \Delta T$ is always positive, it appears most probable that

$$\Delta\phi^*(\text{blend}) > \Delta\phi^*(\text{cryst. comp.})$$

and then in absence of any other effect

$$G(\text{blend}) < G(\text{cryst. comp.})$$

Considering the above, it may be concluded that a mixture of compatible polymers, characterized by the fact that the T_g of the crystallizable component is lower than that of the non-crystallizable component, has a high probability of showing a depression of the radial growth rate of the spherulites.

These conclusions are in agreement with those reported in the literature in the case of PVF_2/PMMA[24] and PCL/PVC[25] mixtures and in the case of PEO/PMMA[26].

Compatible mixtures which verify the condition

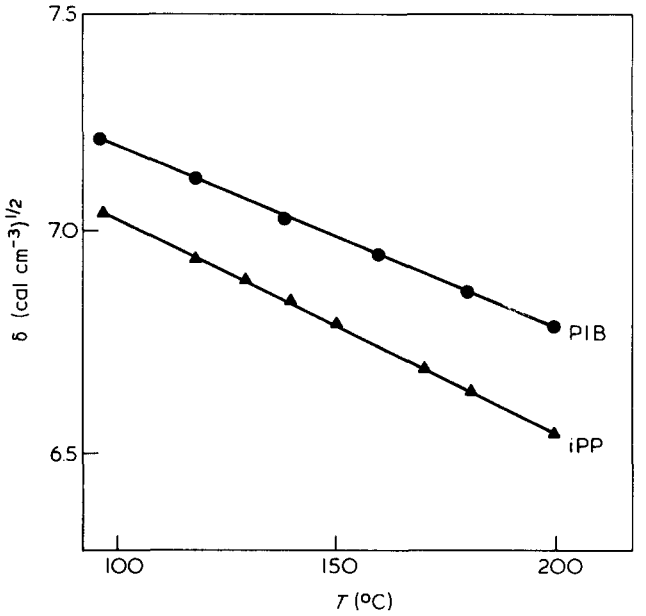

Figure 17 Variation of the solubility parameter δ (cal cm^{-3})$^{1/2}$ with temperature for iPP and PIB

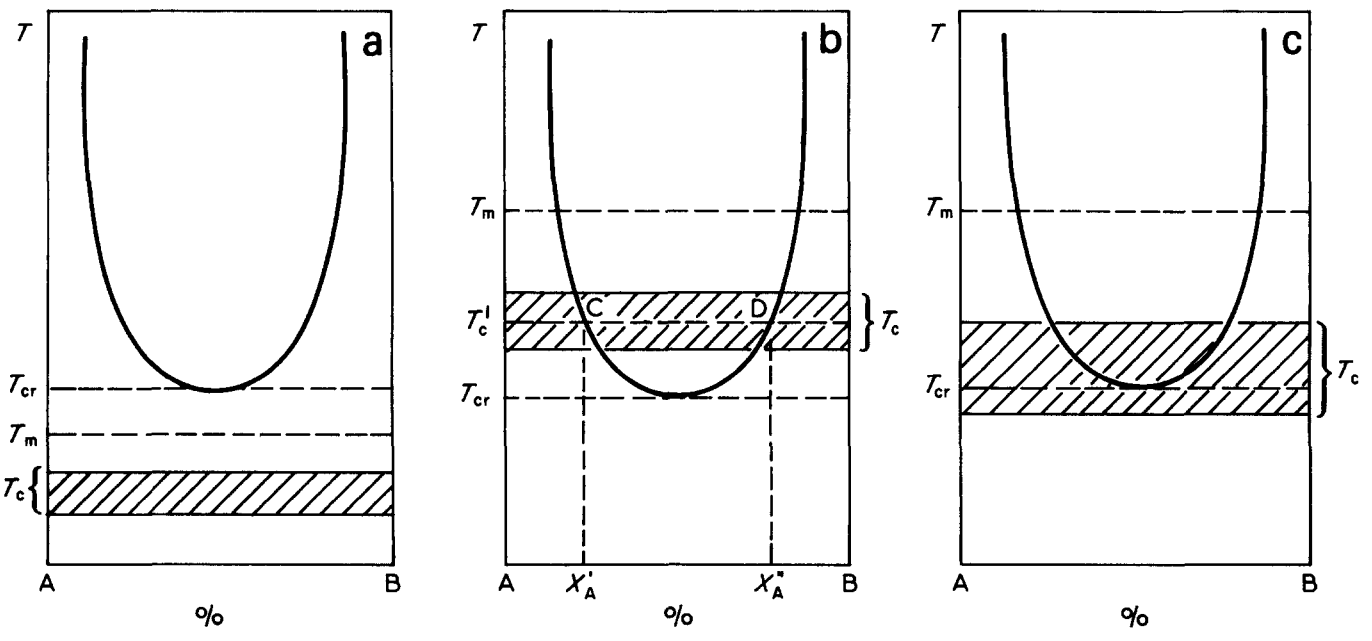

Figure 18 Schematic illustration of phase diagrams of binary blends characterized by a lower critical solution temperature behaviour: (a) compatibility of the components at all T_c and compositions explored; (b) and (c) semicompatibility of the components at the T_c and composition explored

T_g(cryst. comp.) > T_g(uncryst. comp.) may, in principle, also show an increase of G, if the effect of the decrease of ΔF^* is predominant. This could happen at high values of the undercooling where the transport term ΔF^* predominates over $\Delta\phi^*$.

However, it must be underlined that when the content of the uncrystallizable component increases, the entropic term $2\sigma_e k T_m T_c(\ln v_2)/b_o \Delta H \Delta T$ increases and consequently the combined influence of the two terms ΔF^* and $\Delta\phi^*$ may also vary with composition. In this last case a non-monotonic trend of the curves of G *versus* composition, at T_c, or ΔT constant, could be observed.

It may be concluded that the observation of a depression of G, at a given T_c, whose form is an increasing and monotonic function of the uncrystallizable component content in a binary mixture whose polymers verify the conditions T_g(cryst. comp.) < T_g(uncryst. comp.), is probably an indication, together with the depression of the equilibrium melting temperature, of compatibility of the two components in the melt at the T_c and composition explored.

The two polymers, at given T_c *are semicompatible*

According to temperature and composition the crystals may grow in equilibrium with a one-phase or a two-phase melt (see *Figures 18b* and *c*).

Let us assume that the two polymers have a lower critical solution temperature behaviour and the crystallization temperatures explored are higher than the critical temperature (see *Figure 18b*). Increasing the content of the non-crystallizing component (B) because of the diluent effect, the T'_m and T_m of the crystallizable component (A) decrease monotonically until the X'_A composition is reached where phase separation occurs.

At X'_A the system decomposes into the two phases C and D having different compositions: phase C is more rich in the component A whereas phase D is rich in the component B.

Increasing the content of B, the two phases keep their compositions constant until X''_A where the C and D phases disappear. If the two phases C and D are in equilibrium, we should expect no variability of T'_m and T_m as the composition goes from X'_A to X''_A (*Figure 18b*). (It is assumed that phase D is uncrystallizable.)

The minima observed in plots of T'_m and T_m against uncrystallizable component content in iPP/PIB_{HM} and iPP/EPDM systems and in plots of G against composition at constant T_c may probably be explained if it is assumed that during crystallization at T_c the processes of phase separation are followed by molecular fractionation and preferential dissolution of smaller and/or more defective molecules of the crystallizable component in the domains of the uncrystallized polymer. According to this idea phase C will have the same composition on increasing the percentage of B in the blend, but the crystallizable matrix will be made of more perfect molecules and thus the T'_m and T_m would have the opportunity to increase.

The two polymers are incompatible in the melt at the T_c *and composition explored*

The crystals of the crystallizable component grow in equilibrium with its own melt phase. The presence of separate domains of the uncrystallizable component dispersed in the melt matrix during the crystallization process may, because of kinetic effects, influence some matrix quantities, such as the observed melting temperature, crystal and lamellar size, growth rate and crystallinity. A depression of the observed melting point may also be observed; also for these systems plots of T'_m *versus* T_c would be linear; but contrary to what happens in the case of compatibility they will extrapolate to the same T_m value as the pure homopolymer[16].

The morphological factor $1/\gamma$ would be composition-dependent. The presence of domains of the dispersed phase may also produce non-linear rates of growth as these impurities may concentrate between growing spherulites causing, because of physical hindrance, a slow-down of G as a consequence of the fact that the radius of the spherulites at a given T_c is not a linear function of time.

It is interesting to point out that, at least in principle, such kinetic effects may be present even in the case of compatibility between the two components. The predominance of the thermodynamic or kinetic effects may depend in a rather complex way on the temperature and/or the composition.

Some of the synergistic phenomena observed may also be related to the resultant combination of thermodynamic and kinetic effects.

ACKNOWLEDGEMENT

This work was partly supported by Progetto Finalizzato Chimica Fine e Secondaria del CNR, Italia.

REFERENCES

1 Martuscelli, E., Silvestre, C. and Abate, G. C. *Polymer* 1982, **23**, 23
2 Bartczak, Z., Galeski, A. and Martuscelli, E. *Polym. Eng. Sci.*, in press
3 Kumbhoni, K. J. *Polym. Progr. (Plast. Edn.)* 1974 **3** (Aug.–Sept.)
4 Spenadel, L. *J. Appl. Polym. Sci.* 1972, **16**, 2375
5 Karger-Kocsis, J., Kallò, A., Szufner, A., Bodor, G. and Senyei, Zs. *Polymer* 1979, **20**, 37
6 Danesi, S. and Porter, R. S. *Polymer* 1978, **19**, 448
7 Ermilowa, G. A., Ragozina, I. A. and Leont'eva, N. M. *Plast Massy* 1969, **5**, 52
8 Friedrich, K. *Prog. Colloid Polym. Sci.* 1978, **64**, 103
9 Turnbull, D. and Fisher, J. C. *J. Chem. Phys.* 1949, **17**, 71
10 Williams, M. L., Landel, R. F. and Ferry, J. D. *J. Am. Chem. Soc.* 1955, **77**, 3701
11 Boon, J. and Azcue, J. M. *J. Polym. Sci. A-2* 1968, **6**, 885
12 Manaresi, P. and Gianella, V. *J. Appl. Polym. Sci.* 1960, **4**, 251
13 Danusso, F., Moraglio, G., Ghiglia, W., Motta, L. and Todomini, G. *Chim. Ind.* 1959, **41**, 749
14 Eichinger, B. E. and Flory, P. J. *Macromolecules* 1968, **1**, 285
15 Fox, T. G. *Bull. Am. Chem. Soc.* 1956, **2**, 123
16 Hoffman, J. D. *SPE Trans.* 1964, **4**, 315
17 Flory, P. J. 'Principles of Polymer Chemistry', Cornell University Press, Ithaca, 1953
18 Nishi, T. and Wang, T. T. *Macromolecules* 1975, **8**, 909
19 Imken, R. L., Paul, D. R. and Barlow, J. W. *Polym. Eng. Sci.* 1976, **16**, 593
20 Scott, R. L. *J. Chem. Phys.* 1949, **17**, 279
21 Paul, D. R. and Barlow, J. W. in 'Polymer Alloys II' (Eds. D. Klempner and K. C. Frish), Plenum Press, New York, 1980
22 Krause, S. in 'Polymer Blends' (Eds. D. R. Paul and S. Newman), Academic Press, New York, 1978, Ch. 2
23 Hoy, K. L. *J. Paint Technol.* 1970, **42**, 76
24 Nishi, T. and Wang, T. T. *Macromolecules* 1977, **10**, 421
25 Ong, C. J. and Price, F. P. *J. Polym. Sci. Polym. Symp. Edn.* 1978, **63**, 59
26 Martuscelli, E. and Demma, G. in 'Polymer Blends: Processing, Morphology and Properties' (Eds. Martuscelli, Palumbo and Kryszewski), Plenum Press, New York, 1981